Assessment of PV and Wind Microgeneration's Impact in the Power Quality of Low and Medium Voltage Distribution Networks

Paulo Bonifácio, Susana Viana, Luis Rodrigues and Ana Estanqueiro
Portuguese National Laboratory of Energy and Geology - LNEG
Unity of Wind, Solar and Ocean Energy - UESEO
Lisbon, Portugal
ana.estanqueiro@lneg.pt

***Abstract*— Electric power systems face an ever-growing penetration of solar photovoltaic (PV) and other microgeneration as well as non-linear loads such as electric vehicles. There is a common link between these: the extensive use of power electronics converters. These devices are a source of medium–to–high frequency harmonic distortion and their impact on the local distribution grid must be carefully assessed in order to evaluate possible network unbalances, damaging power line resonance conditions, transformer core saturation and overheating.**

Keywords- PV microgeneration; distribution network; power quality)

I. INTRODUCTION

Distributed generation (DG) is an ever-growing reality. As energy price rises, more attractive becomes the option of installing renewable microgeneration in households. Actually, in Portugal, most of the installed microgeneration capacity is solar PV followed by small wind generators.

This new reality presents a challenge to the distribution system operators as power flow is no longer warranted to be always unidirectional, requiring great investments to set adequate protection systems and configure their coordination [1].

The DG production is injected into the local distribution grid using a multitude of DC/AC converters, all of which are built with power electronic commutation devices (e.g. power transistors, IGBTs, GTO Thyristors). These same devices are present in our homes, inside our domestic appliances (e.g. computer power sources, electronic controlled washing machines). Despite being smaller and more efficient than old power converter devices, such new devices present a great drawback: the medium–to–high frequency current distortion harmonics imposed in the distribution networks by their operation.

There must also be considered that most of this DG and non-linear loads are single phase devices connected in a 3 phase system. To this situation one must add the arrival of Electric Vehicles (EV), which are equipped with power electronics converters with a power draw that ranges from 1.2 to 3 kW, the equivalent power of a small household.

As such, the impact of these new stressing conditions on the local distribution grid must be assessed in order to minimize network unbalances and excessive ground currents, brought by uneven power injection/loads in the 3 phases of the network by different kinds of single phase DG/EV devices. Damaging power line resonance conditions, transformer core saturation and overheating brought by harmonic currents must also be carefully evaluated.

This paper presents a methodology developed to access the above described situations; the impact of DG associated power converters, non-linear and common household loads. This work was produced in the scope of the REIVE project [2], in order to access the impact of EVs in the low voltage (LV) distribution network.

A low-medium voltage (LV/MV) power distribution network simulator was developed in Matlab/Simulink. At the core of this simulation an entity was created, the Intelligent Domestic Agent (IDA). The IDA is multi-configurable component, with built-in models for PV/Wind inverters, non-linear and common loads. This agent is used as the base building block in a low voltage power distribution network allowing a swift change in the load and power injection parameters in the line.

In section 2 the simulation models, IDA and low voltage distribution line are introduced. In section 3 the cases considered for the simulation are described and simulation results are presented. Also in this section there is a brief comparison between real PV inverter current signals and the initially used simulation current signals. The conclusions and recommendations of the work are drawn in section 4.

II. SIMULATION MODELS

The basis of the developed methodology to access the relevant aspects associated with the power quality of

The authors would like to thank the REIVE Project coordinators INESC Porto; funded by FAI for partial sponsorship of this paper.

distribution networks is a LV/MV 3 phase balanced/unbalanced power simulator. This simulator integrates models for different power producer/consumer devices that can be commonly encountered in the distribution network. All those models possess a high degree of configurability that allow the user to test different case studies of a same core network without the need to do a deep manual reconfiguration of all the line models.

A. Intelligent Domestic Agent – IDA

At the core of the simulation model there is a reusable, multi-configuration power consumer/producer block that was called the Intelligent Domestic Agent (IDA). This agent supports usual consumer loads, but also possesses more complex models that allow the simulation of multiple types of loads and/or power generation, i.e. PV generation, micro wind generation turbines, nonlinear loads and power storage. Multiple types of IDA can be present at any given time in the simulation without impairing on each other.

Each IDA possesses two types of each model, a physical model and a current injection/consumption model. The physical model is more resource intensive, but allows the assessment of all the generator components and the determination of the line currents and bus voltages. This model allows the simulation and assessment of the variability of the renewable energy resource, i.e.: by feeding solar irradiation and wind speed time series.

In the current injection/consumption model all the fundamental (i.e. 50 Hz) component currents and their relevant harmonics are modelled through ideal current sources allowing the simulation of the interaction of each of the power electronics and non-linear load components of each IDA with the interface of the power grid.

In fig. 1 the block diagram of IDA is presented. This agent is built around 4 main components, a PV generator, a small wind generator, a typical domestic load (i.e. P, Q loads) and a battery charger load. The presence of all or any of the components in any IDA is totally due to user description, thus allowing the simulation to reflect a real-world range of cases.

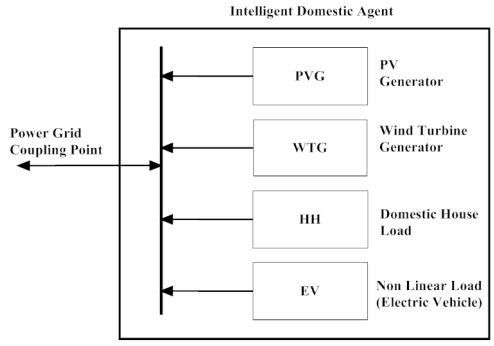

Figure 1. Block diagram of the Domestic Intelligent Agent.

1) Photovoltaic Generator

a) Physical Model

The model works based in meteorological data as an input. The block diagram in fig. 2 shows the proposed PV Generator (PVG) model; this is composed by a subset of 3 different subsystems that interconnect with each other through parameter flow. A current-voltage, I(V), curve generator simulates the PV module response to solar irradiance; a Maximum Power Point Tracker (MPPT) gives optimum power production; finally a DC/AC inverter provides interconnection to the AC grid. The I(V) curve generator receives the ambient temperature (T_{amb}) and global irradiance (G_i) data, then uses this data to generate the PV module current (I_{PV}) that is feed to the MPP tracker. The MPPT feeds optimum voltage (V_{dc}) and current (I_{dc}) data to the DC/AC inverter; from the inverter subsystem outputs the current (I_o) to be injected to the power grid in the Point of Common Coupling (PCC).

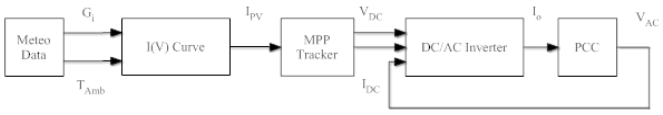

Figure 2. Proposed block diagram for the Photovoltaic Generator (PVG).

b) Current Model

Three sources of current signals for PV inverters where used. A theoretical model developed for the REIVE project [2] and two harmonic current injection models with current signals obtained from the measurement of current signals in active working, grid-tied, solar inverters (<4 kW).

The current signals obtained from the solar inverters, devices (S) and (F), were transformed to the frequency domain with Fast Fourier Transform (FFT). This allowed obtaining the value of each of the current harmonics in the signal spectra, from where the most relevant harmonics to be modelled were selected (i.e. those whose power exceeded 1 W). Sample signals for both (S) and (F) devices are showed in Fig. 3.

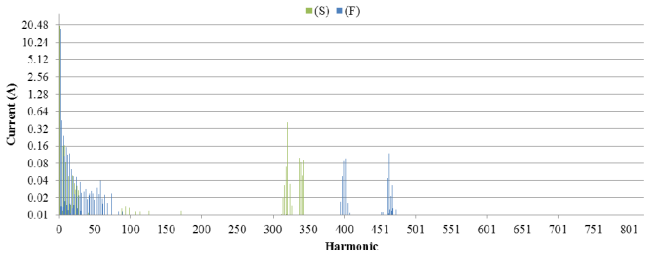

Figure 3. Sample reference signals for (S) and (F) devices.

Following the recommendations of [3] and [4] the microgeneration components were modelled as ideal current sources. These were connected in parallel in a common point with a fundamental current value (at 50 Hz); this later one corresponding to the generated power.

2) Wind Turbine

a) Physical Model

The Wind Turbine Generator (WTG) model is composed of 3 main subsystems. The simulator starts by feeding wind speed data into the rotor/transmission subsystem; from there the mechanical shaft speed parameter (ω_{mec}) is passed to the generator/rectifier subsystem. The rectifier outputs DC voltage and current (V_{dc}, I_{dc}) to the inverter subsystem, which in turn outputs the current (I_o) to be injected in the grid at the PCC.

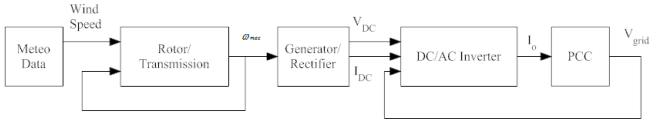

Figure 4. Proposed micro Wind Turbine Generator (WTG).

b) Current Model

The current model for the wind turbine was built in the same way as the current model applied to the PV generator; the currently used data for the wind turbine was obtained from a simulator developed for the REIVE project – Redes Eléctricas Inteligentes com Veículos Eléctricos – Smartgrids with electrical vehicles [2].

3) Battery Charger

a) Physical Model

The proposed battery charger model is built around a low power charger mode. This model corresponds to a typical vehicle on-board charger. The charger operates with a charging rate no greater than 0.1 or 0.2 *C* of the battery power pack capacity (*C*) i.e. for a 25 kWh battery pack the charger supplies a power of 3 to 4 kW to the battery pack [5], [6].

The model is composed of 3 main components; a rectifier connected to a PCC a DC/DC power converter and charge controller which controls the battery charge and the battery pack itself, the proposed model is showed in fig. 5. The AC/DC rectifier takes the voltage (V_{ac}) from a PCC in the power grid, from where it outputs the direct current value (I_{dc}) to the charge controller subsystem; using the voltage and current data from the battery pack, the charge controller generates a charging current (I_{Ch}) which feeds the battery pack.

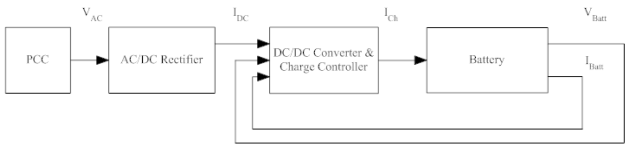

Figure 5. Battery charger physical model (EV).

b) Equivalent Model

The battery charger equivalent model was built following the recommendations of [4] and is based in a parallel *RL* load connected in series with a harmonic current source model, as show in fig. 6. The *R* load represents the battery's active power consumption at nominal frequency; *L* represents the reactive component brought by the charger in partial charge conditions; finally the charger power electronic components are represented by the current sources.

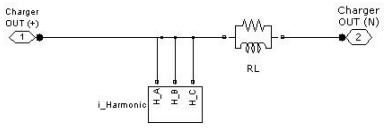

Figure 6. Electric Vehicle charger linear model.

4) House consumer Model

The proposed model for house consumption is composed of a series *RL* load; the *R* value representing the power consumption component (mainly resistive) of the devices connected in the house such as lighting and heating. The *L* value represents the reactive component of the load and is used to model electric motors that are part of some domestic appliances such as blenders or washing machines.

B. Distribution Network Model

The base line used for this work was adapted from a real low voltage 3 phase unbalanced distribution line (400 V_{ac}) were single (230 V_{ac}) and 3 phase users are connected, [7]. Fig. 7 shows the distribution network layout. The network is composed of 6 branches connected to a central power distribution transformer (PT). In each of the branches single and 3 phase users are unevenly connected. In the distribution network diagram, 3 phase loads are represented by (///) with the number (*A*x) corresponding to the quantity of connected users. In the same way single phase users are represented by (//). The doted circle numbers correspond to the bus number and the [*B*] number indicates the connection of the line branch to the power transformer.

Single phase users are considered as common domestic consumers and are represented by a single IDA connected per phase and per bus; 3 phase users are considered as small business or single large domestic users and are represented by a 3 phase load with active and reactive components only (i.e.: no current harmonics injection were considered).

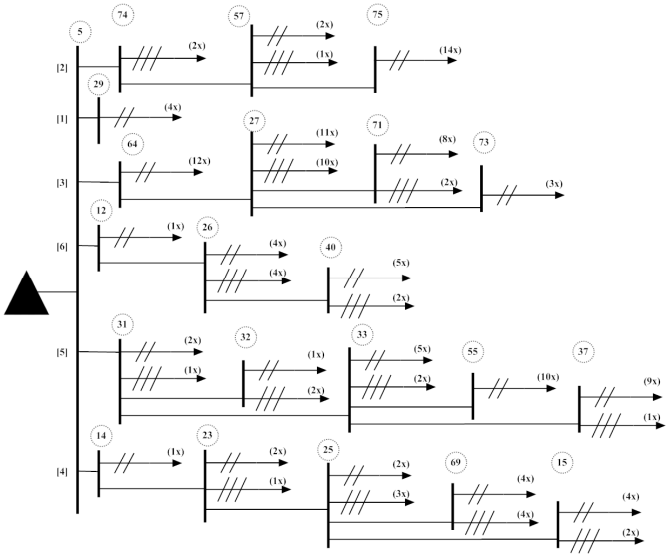

Figure 7. Distribution network diagram used in the simulation.

For simulation purposes, consumers connected to the same bus were aggregated by bus; as a single IDA per phase. In this way a bus with 9 consumers would have 1 IDA per phase (3 in total), each one with the equivalent load for 3 consumers. In cases where the number of consumers didn't allow an even load distribution per IDA (4, 5, 7…) the total load value was divided by the number of consumers with each IDA receiving an uneven part of this load base value (L_{bv}). For a 4 IDA distribution this would correspond to a (2, 1, 1) configuration. L_{bv}, corresponding to two consumers connected to the first phase, and one consumer connected to the other two phases.

This proposed method allows for the simulation of a heavily populated distribution network. The model used was composed of more than 140 consumers.

III. CASE STUDIES AND RESULTS

A. Modelled Case Studies

In order to assess the power quality and harmonic distortion of the distribution grid voltages and currents, 4

case study scenarios were considered. Their parameters are presented in Table I.

TABLE I. TEST SCENARIOS

Case	Conditions	
I	Loads Only	– Full Peak Load
II	Loads	– 25 % Full Peak Load
	EV	– Present in all DIA.
III	Loads	– 25 % Full Peak Load
	EV	– Present in all DIA.
	Microgeneration	– Present in all DIA.
IV	Loads	– 25 % Full Peak Load
	EV	– 1 per bus.
	Microgeneration	– Present in all DIA.

Case I – Full Peak Load – IDAs with Loads Only

The first case scenario considered reflected the technical characteristics of the distribution grid. Peak load power consumption by IDA and grid branch is presented in the appendix.

Case II – 25% of Peak Load – IDAs with Non-Linear Loads

For the second case scenario a part of the peak load value was considered, 25%. All the connected IDAs were enabled with non-linear loads corresponding to EVs.

Case III – 25% of Peak Load – IDAs with Heavy penetration of Non-Linear Loads and Microgeneration

The third case scenario builds on top of the second case; the non-linear loads are complemented with the introduction of some type of microgeneration. A PVG or WTG was placed in the IDAs of each bus. This approach allowed for the evaluation of the impact in the phase current and voltage unbalance, brought by the introduction of microgeneration. Also, the impact on the voltage and current distortion caused by the introduction of microgeneration sources together with the heavy penetration of EVs could be evaluated.

Case IV – 25% of Peak Load – IDAs with some Non-Linear Loads and Heavy Penetration of Microgeneration.

The final test scenario considered the conditions of the 3rd Case and added microgeneration. EV penetration was reduced to 1 EV per bus in order to lower their impact in the simulation. This option was chosen in order to assess the voltage dip prevention and grid stabilization capability brought by microgeneration sources.

B. Results

Values for the Voltage and its Total Harmonic Distortion (THD_v) in the low voltage, secondary side of the power transformer are presented for all considered cases. To perform the current analysis and its Total Harmonic Distortion (THD_i), measurements were taken at the branches 1 to 6 in the low voltage side of the power transformer. These branches are as follows:

- Branch 1 – between bus 5 and bus 29.
- Branch 2 – between bus 5 and bus 75.
- Branch 3 – between bus 5 and bus 71.
- Branch 4 – between bus 5 and bus 15.
- Branch 5 – between bus 5 and bus 55.
- Branch 6 – between bus 5 and bus 40.

Next the values of the voltages in the most distant points of the line for each branch and its corresponding line were taken; the line location is as follows:

- Line 0 – from the secondary of the PT to bus 5.
- Line 1 – from bus 5 to bus 29.
- Line 2 – from bus 57 to bus 75.
- Line 3 – from bus 27 to bus 71.
- Line 4 – from bus 25 to bus 15.
- Line 5 – from bus 33 to bus 55.
- Line 6 – from bus 26 to bus 40.
- Line 7 – from bus 64 to bus 27.
- Line 8 – from bus 25 to bus 69.

Line 7 and 8 don't correspond to the most distant lines from the PT, but were included as they present points of interest as the most heavily loaded buses of the low voltage distribution network.

For case III and IV the used current signals were augmented with signals obtained from two different grid-tied solar inverters, (S) and (F), both in the 4 kW power range. For analysis purposes data is shown in detail for selected lines and buses.

1) *Voltages at the secondary side of the Power Transformer and currents in line 0*

In fig. 8 it can be observed that in the cases I to III the voltage at the secondary of the PT oscillate between 0.992 and 0.996 *per unit* (p.u.) in all 3 phases. In case IV the voltage is very close to 1 p.u. oscillating between 0.998 and 0.999 p.u.. Regarding the THD_v as the penetration of microgeneration and EVs is increased, so does the distortion , as seen in the cases I to III. In case IV the reduction of loads from EV sources more than doubles the voltage distortion seen across all the 3 phases.

Fig. 9 shows the values and distortion of the current on the 3 phases. Some current unbalance can be seen in cases I and II. With the introduction of microgeneration the nature of the unbalance changes, as more current flows in phase 2 and 3 in comparison to phase 1 and as opposed to what is seen in the first two cases. But the most notorious effect occurs in the neutral current as values spike up in case III and IV. The current distortion increases with the addition of EV and microgeneration in cases I to III. In case IV the reduction of EVs also leads to an increase of THD_i, this situation seems to indicate an attenuation of distortion brought by the load of the EV.

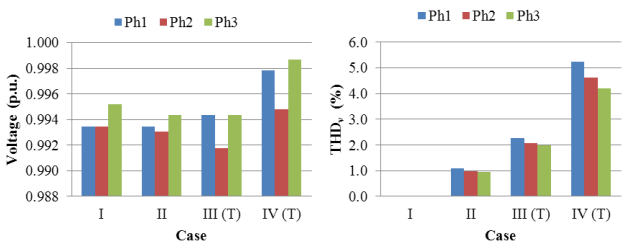

Figure 8. Voltage and voltage distortion (THD_v) at bus 5.

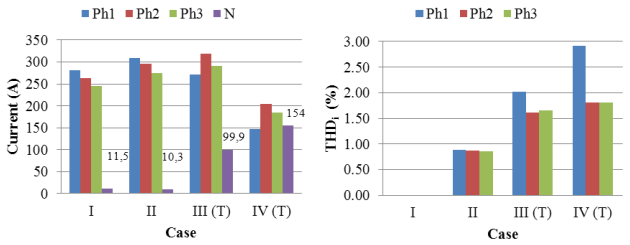

Figure 9. Current and current distortion per phase and in the neutral measured at line 0. (Note that the neutral current distortion is not presented).

Fig. 10 represents a typical signal obtained from the simulation in the low voltage side of the power transformer.

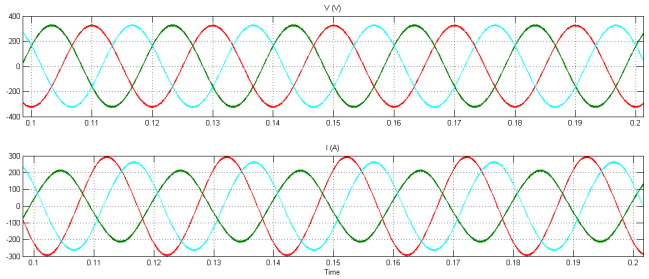

Figure 10. Voltage at the low voltage side of the PT and current in line 0, for case IV(T).

Tables II and III present the simulation results for the voltage at bus 5 and current at line 0 of the distribution network. Analysing the data from both tables it can be noted that the introduction of microgeneration was useful in increasing the voltage at bus 5. Also it's noteworthy that the association of microgeneration with EVs reduced the current thought the line branches. On the other side this same association reduced the current distortion (THD_i) but increased the measured voltage distortion (THD_v) in cases III and IV.

TABLE II. VOLTAGE AND THD_V AT LOW VOLTAGE SIDE OF THE POWER TRANSFORMER

Case	Bus 5					
	Ph1		*Ph2*		*Ph3*	
Voltage	*V (p.u.)*	*THD_v (%)*	*V (p.u.)*	*THD_v (%)*	*V (p.u.)*	*THD_v (%)*
I	0,993	0,00	0,993	0,00	0,995	0,00
II	0,993	1,09	0,993	0,99	0,994	0,96
III(T)	0,994	2,28	0,992	2,06	0,994	2,00
III(S)	0,994	1,75	0,992	1,58	0,995	1,54
III(F)	0,994	1,51	0,992	1,38	0,995	1,32
IV(T)	0,998	5,23	0,995	4,62	0,999	4,19
IV(S)	0,998	1,62	0,994	1,41	0,999	1,26
IV(F)	0,998	1,26	0,994	1,06	0,999	0,92

TABLE III. CURRENT AND THD_I AT LINE 0

Case	Line 0						
	Ph1		*Ph2*		*Ph3*		*N*
Current	*I (A)*	*THD_i (%)*	*I (A)*	*THD_i (%)*	*I (A)*	*THD_i (%)*	*I (A)*
I	281,50	0,00	262,90	0,00	245,80	0,00	11,51
II	309,30	0,88	295,10	0,87	274,60	0,86	10,34
III(T)	270,90	2,02	318,10	1,61	291,70	1,65	99,89
III(S)	264,50	1,78	321,70	1,37	295,40	1,38	118,80
III(F)	266,80	2,88	320,60	2,25	294,60	2,26	112,60
IV(T)	147,70	2,91	204,90	1,81	184,90	1,81	154,50
IV(S)	141,10	2,63	213,80	1,50	194,30	1,49	184,00
IV(F)	143,30	4,63	210,70	2,81	191,10	2,81	174,10

Neutral currents due to phase imbalance start to be noted with the introduction of EV loads and rise with a heavy penetration of microgeneration, cases (II/III/IV).

Comparing the results obtained with the measured current signals, in case III/(S)/(F) and IV/(S)/(F), it can be noted that the harmonic current content of the power electronics devices that build-up the solar power inverters have a significant impact in the voltage and current distortion measured in the bus/line. In cases IV(S) and IV(F), the later THD_i is higher than the former; 4.63% versus 2.63%, for phase 1. As for the THD_v the situation inverts, as IV (S) has a greater measured distortion than IV(F); 1.26% versus 1.62%.

These results can be explained by the line impedance diagram (fig. 11) and the lines distance to the PT. As lower frequency harmonic currents face lower equivalent impedance, they tend to propagate through the network. On the other side, higher frequency harmonics currents face a higher impedance, tending to be transduced into voltage harmonics and not propagating as much as lower frequency currents. As impedances are distributed throughout the length of the lines, the line distance to the transformer also plays a role in the harmonic propagation in a network. The longest distance to the power transformer occurs in line 3; bus 71 whose connection is placed at 463 m from the PT. This distance does not allow for the complete dissipation of the low power harmonics; additionally, for frequencies higher than 10 kHz line impedance rises above 1 ohm reinforcing the impact of high frequency current harmonics in voltage distortion.

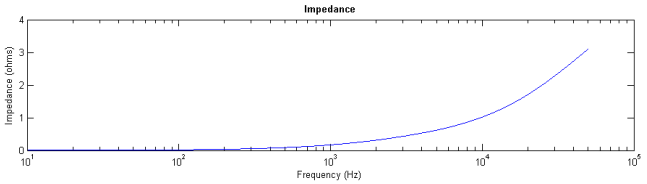

Figure 11. Distribution network line impedance for phase 1.

Analysing the sample signals in fig. 3 it can be seen that there is some difference between both devices. The measured harmonic content for device (S) had the most harmonic power above the 10 kHz range, (0.2 A at 20 kHz). Device (F) had more powerful 3rd and 7th harmonics but a lower power 399th harmonic, 0.45 A, 0.25 A and 0.13 A for the 3rd, 7th, and 399th harmonic, respectively.

2) Branch 3: Voltages at bus 27 and 71; currents in line 7 and 3

Branch 3 is one of heaviest loaded branches of the distribution network. Results are show for the longest and the heaviest loaded buses. At bus 71 (fig. 12) the most distant point from the PT; the use of microgeneration helps to enhance the voltage level at that location with values above 0.90 p.u. for each of the 3 phases. There is a trade off in the form of measured THD_v, that has a slight increase, although this value is still under current normative values for voltage distortion (EN 51160 and IEC 61000-2-2 standards) [8], [9].

Fig. 13 shows the current through line 3. A slight current unbalance can be seen, and it becomes more significant with the elimination of EVs from the model (case IV). When we look at the most loaded bus of branch 3; bus 27, line 7; the

impact of microgeneration to assist in low voltage levels situation becomes evident. Case I has a peak load scenario and can only be used as reference. Cases II to IV present a load scenario of 25 % of the peak load, enabling to assess the impact of the use of microgeneration and the penetration of EV loads in the power quality of the local grid.

In fig. 13 the introduction of microgeneration enhances the average voltage but adds some THD_v. Voltage values are constantly above 0.93 p.u. for case IV and close to 0.90 p.u. in case III.

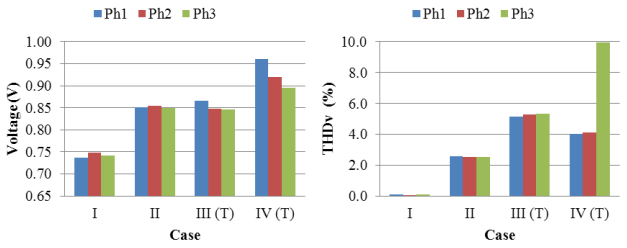

Figure 12. Voltage at bus 71 of branch 3..

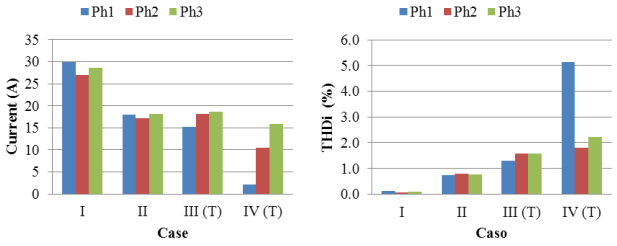

Figure 13. Current flow through line 3 of branch 3.

In Fig. 14, the uneven distribution of loads and microgeneration becomes apparent for case IV with a significant current unbalance for phase 2 relatively to phases 1 and 3. All these unbalances dispersed throughout the distribution network account for the neutral current values that are shown in table III.

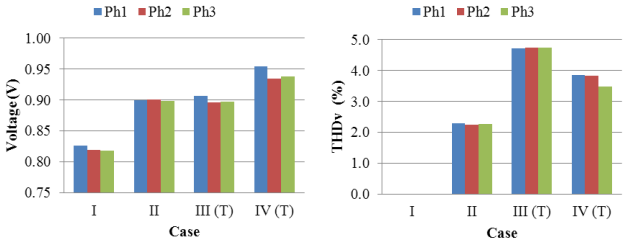

Figure 14. Voltage at bus 27 of branch 3.

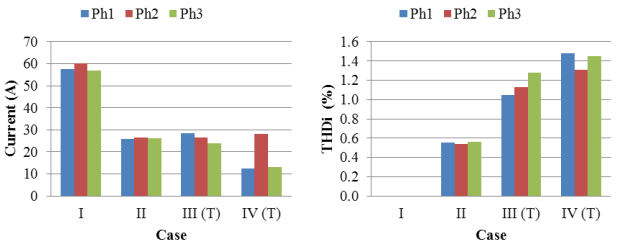

Figure 15. Current flow through line 7 of branch 3.

C. *Current and Voltage Distortion Limits According to Normative Standards*

Normative standards for total harmonic distortion of current (THD_i) values are specified by IEC 61000-3-2 and are defined by equipment class. The maximum allowed current distortion supplied by the distribution network cannot exceed 15 %, [10] and [11]. At this time there is no specified normative that stipulates the maximum value of injected current distortion into the grid.

This distortion value is calculated with harmonic values of up to the 40th harmonic, 2000 Hz.

For the voltage, total harmonic distortion values (THD_v) are specified by standard IEC 61000-2-2. With harmonic values of up to the 50th harmonic and must not exceed a THD_v of 8%, [9].

Fig. 16 and 17 show the same voltage signal; bus 5, phase 1; with and without normative constrains.

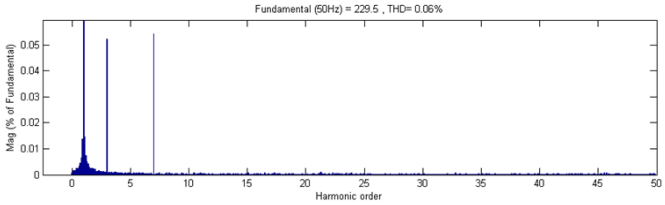

Figure 16. Voltage distortion with normative values, at bus 5, phase 1, for case IV(F).

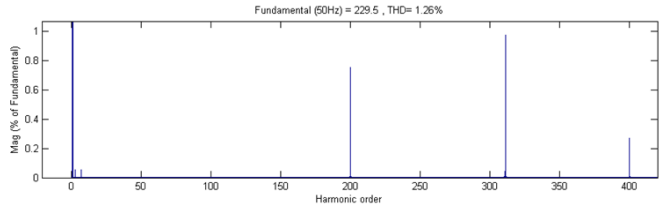

Figure 17. Voltage distortion with maximum injected harmonic spectrum; at bus 5, phase 1 for case IV(F).

When only the normative harmonic values are considered THD values are always according to normative constrains. When the measurements range is expanded there is a noticeable increase in measured distortion, both in voltage and current. From [1] where extracted line resonance values that varied from 14 to 17 kHz. Also measured harmonic values for devices (S) and (F) varied not only in current values but also in frequency according to total solar irradiance; with harmonics ranging from 300th to 470th (fig. 3). This situation is characteristic of switching power components that vary their duty cycle according to load and available power.

Some of this harmonics can occur on top of the line resonance conditions and a damaging event can occur in the distribution network.

IV. CONCLUSIONS AND RECOMMENDATIONS

This paper presented a methodology to assess the impact of distributed microgeneration and non-linear loads in the power quality (harmonics) of low voltage local distribution network. This was achieved with the introduction of a simulation tool composed of physical and harmonic current models for all of the different network components. These current signals can be obtained from local database signals or from signals obtained from external simulation of physical models for each component.

The simulation results show that in the case of unbalanced 3 phase low voltage networks; caution must be taken when placing a representative number of

microgeneration's sources, as each source placement can deteriorate the line balance.

Results suggest that a pre-normative recommendation should be made in order to allow a greater number of harmonics to be taken into account when calculating THD values: as it has been shown, harmonic current and voltage can appear near or on top of line frequency resonance, with dangerous consequences for grid operation and most of the connected equipment. Also, it must be considered that the ever-increasing penetration of low quality medium sized switch-mode power supplies (<1kW) in an domestic environment, can lead to a growth of situations of line distortion.

ACKNOWLEDGMENTS

The authors would also like to extend their tanks to Eng. Maria João Martins from LNEG for her help in acquiring the current signals from the grid-tied solar inverters used in the simulation.

REFERENCES

[1] P. Bonifácio, S. Viana, M. J. Martins and A. Estanqueiro, "Projecto REIVE, Tarefa 2 - Desenvolvimento de Ferramentas de Análise de Impacto Técnico da Integração de Microgeração e Veículos Eléctricos.," LNEG, Lisboa, 2012.

[2] Projecto REIVE, Available: http://www.lneg.pt/iedt/projectos/264/. [Accessed: May 2012].

[3] IEEE - Task Force on Harmonics Modeling and Simulation, "Modeling and Simulation of the Propagation of Harmonics in Electric Power Networks Part I : Concepts, Models and Simulation Techniques," IEE Transactions on Power Delivery, vol. 11, January 1996.

[4] IEEE - Task Force on Harmonics Modeling and Simulation, "Modeling and Simulation of the Propagation of Harmonics in Electric Power Networks Part II : Sample Systems and Examples," *IEE Transactions on Power Delivery,* vol. 11, January 1996.

[5] T. Olivier and D. Louis-A., "Experimental Validation of a Battery Dynamic Model for EV Applications," *World Electric Vehicle Journal,* vol. 3, no. EVS24, 2009.

[6] Kuperman, A.; Levy, U.; Goren, J.; Zafranski, A.; Savernin, A.; , "High power Li-Ion battery charger for electric vehicle," Compatibility and Power Electronics (CPE), 2011 7th International Conference-Workshop , vol., no., pp.342-347, June 2011.

[7] P. Bonifácio, S. Viana, L. Rodrigues and A. Estanqueiro, "Projecto REIVE - Tarefa 3 – Teste e Optimização de Ferramentas de Análise da Qualidade de Energia e Distorção Harmónica," LNEG, Lisboa, 2012.

[8] EN 50160: 2006, "Voltage characteristics of electricity supplied by public distribution systems".

[9] IEC 61000-2-2: 2002 (Ed. 2.0),"Electromagnetic compatibility (EMC) - Part 2-2: Environment - Compatibility levels for low-frequency conducted disturbances and signalling in public low-voltage power supply systems".

[10] EN 50438: 2007 (Ed. 1), "Requirements for the connection of micro-generators in parallel with public low-voltage distribution networks".

[11] IEC 61000-3-2 : 2009 (Ed. 3.2), "Electromagnetic compatibility (EMC) – Part 3-2: Limits – Limits for harmonic current emissions (equipment input current ≤16 A per phase)"

.

V. APPENDIX – I

A. Current and THDi per branch

Tables V to X present the measured current and THD_i in selected branches connected to the low voltage side of the power transformer.

TABLE IV. CURRENT AND THD_I AT BRANCH 3

Case	Branch 3					
	Ph1		*Ph2*		*Ph3*	
Current	*I (A)*	*THD_i (%)*	*I (A)*	*THD_i (%)*	*I (A)*	*THD_i (%)*
I	90,87	0,00	90,51	0,00	88,14	0,00
II	75,94	0,76	76,84	0,76	79,10	0,76
III(T)	68,46	1,52	80,50	1,53	80,54	1,56
III(S)	70,50	1,29	81,75	1,23	81,94	1,34
III(F)	69,81	1,86	81,32	2,33	81,46	2,34
IV(T)	44,09	1,88	48,96	1,8	48,3	1,78
IV(S)	46,66	1,49	51,84	1,57	51,61	1,54
IV(F)	45,79	2,32	50,85	3,10	50,48	3,09

TABLE V. CURRENT AND THD_I AT BRANCH 4

Case	Branch 4					
	Ph1		*Ph2*		*Ph3*	
Current	*I (A)*	*THD_i (%)*	*I (A)*	*THD_i (%)*	*I (A)*	*THD_i (%)*
I	67,85	0,00	56,33	0,00	51,10	0,00
II	71,55	0,83	69,33	0,83	56,85	0,84
III(T)	64,64	1,93	75,47	1,47	61,24	1,51
III(S)	61,92	1,79	76,14	1,30	61,08	1,28
III(F)	62,83	3,08	75,91	2,11	61,14	1,93
IV(T)	36,06	2,66	53,11	1,76	38,84	1,59
IV(S)	33,25	2,70	54,13	1,47	39,61	1,30
IV(F)	34,19	4,96	53,78	2,57	39,35	2,29

TABLE VI. CURRENT AND THD_I AT BRANCH 5

Case	Branch 5					
	Ph1		*Ph2*		*Ph3*	
Current	*I (A)*	*THD_i (%)*	*I (A)*	*THD_i (%)*	*I (A)*	*THD_i (%)*
I	45,22	0,00	44,13	0,00	43,75	0,00
II	61,07	0,92	62,04	0,92	64,55	0,90
III(T)	50,43	2,20	67,26	1,80	71,62	1,60
III(S)	49,43	1,93	68,94	1,52	72,19	1,36
III(F)	49,77	3,03	68,36	2,65	72,00	2,11
IV(T)	23,1	3,81	42,19	2,06	50,63	1,88
IV(S)	21,77	3,45	46,81	1,75	51,64	1,54
IV(F)	22,21	5,95	45,23	3,46	51,29	2,62

TABLE VII. CURRENT AND THD_I AT BRANCH 6

Case	Branch 6					
	Ph1		*Ph2*		*Ph3*	
Current	*I (A)*	*THD_i (%)*	*I (A)*	*THD_i (%)*	*I (A)*	*THD_i (%)*
I	39,66	0,00	34,59	0,00	28,02	0,00
II	50,59	1,00	35,97	0,93	35,83	0,96
III(T)	44,00	2,42	39,02	1,60	38,29	1,90
III(S)	41,73	2,14	38,99	1,34	39,34	1,93
III(F)	42,49	3,48	39,06	1,78	38,98	2,53
IV(T)	10,44	7,12	28,06	1,8	25,54	2,09
IV(S)	7,13	9,64	27,87	1,33	26,83	1,73
IV(F)	8,23	15,15	27,93	1,97	26,39	3,20

B. Line and Client Data

TABLE VIII. LOAD DISTRIBUTION BY CONSUMER

Branch	Peak Load			Single Phase						3 Phase	
	P (kW)	*Q (kVAr)*	*Consumers*	*P1*	*P2*	*P3*	*Q1*	*Q2*	*Q3*	*P*	*Q*
1	1,9	0,76	4	0,95	0,48	0,48	0,38	0,19	0,19	--	--
	2,6	1,04	2	--	--	--	--	--	--	2,60	1,04
2	2,9	1,16	3	0,97	0,97	--	0,39	0,39	--	0,97	0,39
	18	7,2	14	6,43	6,43	5,14	2,57	2,57	2,06	--	--
	9,3	3,72	12	3,10	3,10	3,10	1,24	1,24	1,24	--	--
3	36,2	14,48	21	6,90	6,90	5,17	2,76	2,76	2,07	17,24	6,90
	15,1	6,04	11	5,49	4,12	4,12	2,20	1,65	1,65	1,37	0,55
	5,2	2,08	3	1,73	1,73	1,73	0,69	0,69	0,69	--	--
	0,4	0,16	1	0,40	--	--	0,16	--	--	--	--
	2,3	0,92	3	0,77	0,77	--	0,31	0,31	--	0,77	0,31
4	8,9	3,56	5	1,78	1,78	--	0,71	0,71	--	5,34	2,14
	17,9	7,16	8	4,48	2,24	2,24	1,79	0,90	0,90	8,95	3,58
	11,6	4,64	6	3,87	1,93	1,93	1,55	0,77	0,77	3,87	1,55
	5,6	2,24	3	1,87	1,87	--	0,75	0,75	--	1,87	0,75
	6,7	2,68	3	2,23	--	--	0,89	--	--	4,47	1,79
5	6,6	2,64	7	1,89	1,89	0,94	0,75	0,75	0,38	1,89	0,75
	4,2	1,68	10	1,26	1,26	1,26	0,50	0,50	0,50	0,42	0,17
	8,1	3,24	10	3,24	2,43	2,43	1,30	0,97	0,97	--	--
	0,4	0,16	1	0,40	--	--	0,16	--	--	--	--
6	9,6	3,84	8	2,40	1,20	1,20	0,96	0,48	0,48	4,80	1,92
	13,9	5,56	7	3,97	3,97	1,99	1,59	1,59	0,79	3,97	1,59
Total	187,4	74,96	142	54,11	43,05	31,73	21,64	17,22	12,69	58,51	23,40

TABLE IX. POWER TRASNFORMER DATA.

Power Transformer (PT)	
S (kVA)	400
U_{MV} (kV)	15
U_{LV} (V)	400
R transformer (Ω)	0,00378
X transformer (%)	6%

TABLE X. BRANCH AND LINE DATA

Branch	*Bus*		*Length*	*Phase & Neutral*	
	From	*To*	*(m)*	*R (Ω/km)*	*X (Ω/km)*
1	5	29	40	0,496	477,5E-6
	5	74	180	0,857	477,5E-6
2	74	57	95	1,300	477,5E-6
	57	75	156	2,942	455,3E-6
	5	64	105	0,202	318,3E-6
3	64	27	250	1,025	358,7E-6
	27	71	108	2,191	386,4E-6
	27	73	33	2,463	392,4E-6
	5	14	20	0,393	318,3E-6
	14	23	141	0,438	387,5E-6
4	23	25	132	0,695	428,0E-6
	25	69	102	1,303	440,8E-6
	25	15	168	1,841	451,7E-6
	5	31	126	2,627	378,9E-6
	31	32	20	3,361	392,4E-6
5	31	33	134	2,534	433,1E-6
	33	37	128	2,454	389,6E-6
	33	55	78	2,473	370,2E-6
6	5	12	78	1,067	318,3E-6
	12	26	152	1,522	459,5E-6
	26	40	93	2,463	464,7E-6

As no data was available for line capacity (C); the same value as stated in [1] was used; $C = 0.6 \times 10^{-9}$ F/km.